Color and luminance asymmetries in the clear sky

Javier Hernández-Andrés, Raymond L. Lee, Jr., and Javier Romero

A long-standing assumption about the clear sky is that its colors and luminances are distributed symmetrically about the principal plane. As useful as this approximation is, our digital-image analyses show that clear-sky color and luminance routinely depart perceptibly from exact symmetry. These analyses reconfirm our earlier measurements with narrow field-of-view spectroradiometers [J. Opt. Soc. Am. A **18,** 1325 (2001)], and they do so with much higher temporal and angular resolution across the entire sky dome. © 2003 Optical Society of America

OCIS codes: 010.1290, 330.1710, 330.1730.

1. Introduction

One of the oldest assumptions about cloudless skies is that their chromaticity and luminance distributions are symmetric about the solar meridian, or principal plane. Assuming that skylight exhibits macroscopic symmetry follows logically from the microscopic scattering symmetry of single molecules or collections of randomly oriented aerosols. Skylight symmetry also agrees with the evidence of our eyes—the clear daytime sky's color and brightness indeed look balanced on either side of the principal plane. But what experimental evidence exists for this symmetry?

Across several decades and with a variety of goals, numerous researchers have studied the angular distribution of the clear daytime sky's visible-wavelength radiances. One consequence of this diverse research is a variety of empirical and theoretical models of clear-sky radiance and luminance across the sky dome.[1–5] Although the clear sky's patterns of spectra and chromaticities merit as much attention as its radiance patterns, little experimental research has been done on the former,[6–9] because quickly mapping the entire sky was, until recently, a difficult feat.

Physically realistic models of the clear sky's color

J. Hernández-Andrés (javierha@ugr.es) and J. Romero are with the Departamento de Óptica, Facultad de Ciencias, Universidad de Granada, Granada 18071, Spain. R. L. Lee, Jr. is with the Mathematics and Science Division, United States Naval Academy, Annapolis, Maryland 21402.

Received 8 January 2002; revised manuscript received 25 March 2002.

distributions also have been relatively rare. A notable exception comes from Sekine, who in 1991 calculated theoretical clear-sky chromaticities along the solar meridian.[10] Sekine analyzes how aerosol optical depth, solar elevation, scattering angle, and reflected surface light all affect sky color. He shows that, for constant solar elevation, moving along the solar meridian generates V-shaped chromaticity curves for skylight. Furthermore, these Vs nearly parallel the Planckian locus on its green side, i.e., above the Planckian locus. Although Sekine's analysis is a useful start, it is restricted to the solar meridian and thus can offer no insights into clear-sky color symmetry.

In 1994, one of us (Lee) used digital image analysis to measure daytime and twilight clear-sky chromaticities along several different meridians near the horizon.[11,12] This technique produced data comparable in quality with that derived from spectroradiometers, with the added advantage of having quite high angular and temporal resolution. Among other conclusions, this study showed that clear daytime skies have purity minima a small distance above, rather than at, the astronomical horizon. Now we quite literally expand our horizons by applying an improved version of this digital-image analysis to the entire hemisphere of the clear sky.

2. Previous Research on Skylight Asymmetries

Recently we analyzed ~1600 skylight spectra acquired during a 7-month period in Granada, Spain (37° 11′ N, 3° 35′ W, altitude 680 m).[13] These clear-sky spectral radiances were measured within 3° fields of view (FOVs) along four sky meridians: the solar meridian with relative azimuth $\phi_{rel} = 0°$, and three meridians at $\phi_{rel} = 45°$, 90°, and 315° to it. Note that ϕ_{rel} increases clockwise from the Sun's az-

imuth (i.e., ϕ_{rel} increases in the same sense as compass direction).

When we reuse our earlier notation,[13] view-elevation angle h increases from 0° at the astronomical horizon to $h = 90°$ at the zenith. If skylight symmetry holds true, then we should observe the same chromaticity and luminance at any symmetric pair of viewing directions h, $\phi_{rel} = 180° \pm \Delta\phi$, where $0° < \Delta\phi < 180°$. Thus $h = 20°$ and $\phi_{rel} = 30°$, 330° are one such pair of *geometrically symmetric view* (GSV) directions; $h = 60°$ and $\phi_{rel} = 95°$, 265° are another GSV pair. Although any given pair of GSV directions has the same scattering angle from the Sun, the fact that two viewing directions have equal scattering angles does not mean in general that they are a GSV pair.

A significant constraint on our Granada radiometer measurements was that we could measure only a relatively few radiances (44 in total) across the entire sky quickly enough that unrefracted Sun elevation h_0, and thus scattering geometry, changed negligibly. One salient result from our measurement campaign[13] suggests that Sekine's model[10] may be a special case of a more general phenomenon. Namely, most of our scans along the four sky meridians yielded distinctly V-shaped chromaticity curves, and these Vs nearly coincide with the Commission Internationale de l'Eclairage (CIE) daylight locus.

Yet even with only 44 radiances per h_0, our earlier skylight analysis routinely found perceptible chromaticity and luminance differences in various GSV directions. Independent of h_0, color asymmetries in GSV pairs often exceeded 1 just-noticeable difference[14] (JND), reaching a maximum of 4.5 JNDs. Given that clear-sky color and luminance are closely linked at a given h_0, not surprisingly we also found luminance asymmetries about the principal plane. With a 2% luminance difference as a typical threshold for photopic vision, almost all GSV directions had perceptible luminance differences.

3. Are Skylight Asymmetries Real, or Are They Measurement Artifacts?

Despite (or perhaps because of) the fact that these asymmetries occur routinely, a fair question is whether they are real or are merely artifacts caused by our measurement technique or by the spectroradiometer itself. One obvious quibble involves the time required for making our meridional measurements. Indeed, some of the observed asymmetries might be ascribed to the 4 min needed for our LI-COR LI-1800 spectroradiometer[15] to survey the entire sky. However, our uncertainty in measuring ϕ_{rel} was comparable in magnitude with changes in solar position during this period. Thus we reasoned that changes in solar elevation and azimuth may slightly increase but would not cause the observed color and luminance asymmetries.

Strong support for this reasoning comes from skylight measurements made with a faster spectroradiometer, a Photo Research PR-650[16] with a 1° FOV. Even though this instrument lets us acquire spectra from two GSV directions as quickly as we can reaim it ($\sim$5–7 s), we still found perceptible differences in skylight. However, to address definitively the question of temporal changes in clear-sky color and luminance, we now turn to a technique that offers far higher angular and temporal resolution—digital analysis of fish-eye photographs.

4. Digital-Image Analysis of Fish-Eye Photographs

Whether derived from digital cameras or scanned film, the inherent advantage of digital images is that their angular and temporal resolutions can be quite small: Here each pixel subtends a linear angle of $\sim$0.3° (solid angle $\sim$2.2 $\times$ 10^{-5} sr), and images are acquired in 1/125–1/4 s (depending on h_0). As with our earlier spectroradiometer measurements, we took our fish-eye photographs in Granada, Spain. Although our observing site's horizon has few topographic obstructions, these nonetheless give us unambiguous compass directions, which in turn let us calculate ϕ_{rel} accurately. As a result, our uncertainty in determining azimuths is 1°, as described in Ref. 13. Our visual prerequisite for taking measurements was that the sky must appear to be completely cloudless.

We photographed the entire sky at different h_0, using a Nikkor 8-mm objective[17,18] (FOV = 180° or 2π sr), and we aimed the optical axis of the lens at the zenith. To avoid exposure problems and lens flare during the day, we shaded the camera lens from direct sunlight with a small disk attached to a thin pole. After scanning fish-eye photographs of the sky and of a color-calibration card, we began our digital-image analysis. When we photographed the color-calibration card, it was illuminated by daylight (skylight plus direct sunlight) with a known spectral power distribution. Because we are interested only in measuring chromaticities of the *convolved* spectra of skylight illuminants and scatterings, our known daylight illuminant need not be (and in general will not be) identical to those that illuminate scatterers at different altitudes in the clear sky. Lee describes in detail the calibration procedure for, and advantages and limitations of, his particular technique.[12] It is especially useful in calculating relative chromaticities and luminances for different light sources. That is certainly our task here, since we are comparing color and brightness differences for many different pairs of clear-sky GSV directions.

For each digital image we use our colorimetric calibration algorithm to map red–green–blue pixel gray levels into CIE 1931 x, y chromaticities and relative luminance Y. Instead of calculating color and luminance differences directly from x, y, and Y in the perceptually anisotropic CIE XYZ color space, we first map this data into the isotropic CIELUV color space.[14,19] Within this space we calculate the CIELUV color difference ΔE^*_{uv}, which for any pair of clear-sky GSV directions is

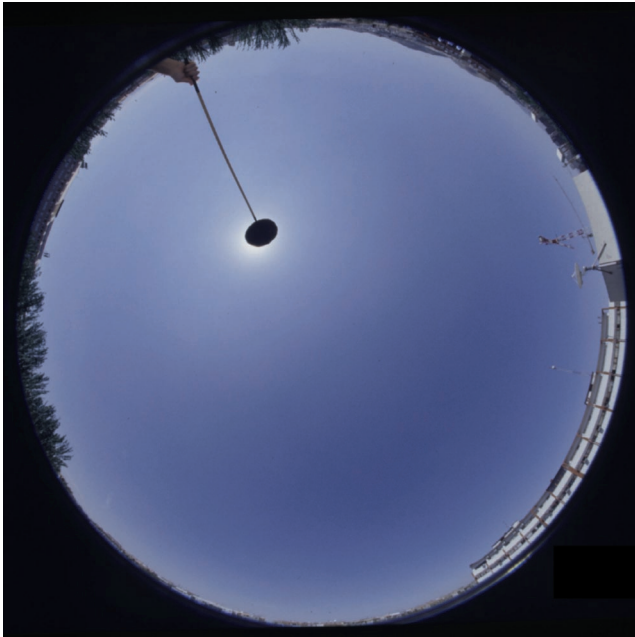$$\Delta E^*_{uv} = [(\Delta L^*)^2 + (\Delta u^*)^2 + (\Delta v^*)^2]^{1/2} \, .$$

Fig. 1. Fish-eye photograph of a clear sky in Granada, Spain, on 21 May 2000 at 10:24 UTC. Unrefracted solar elevation $h_0 = 60.0°$ above the astronomical horizon, and the photograph is centered on the zenith.
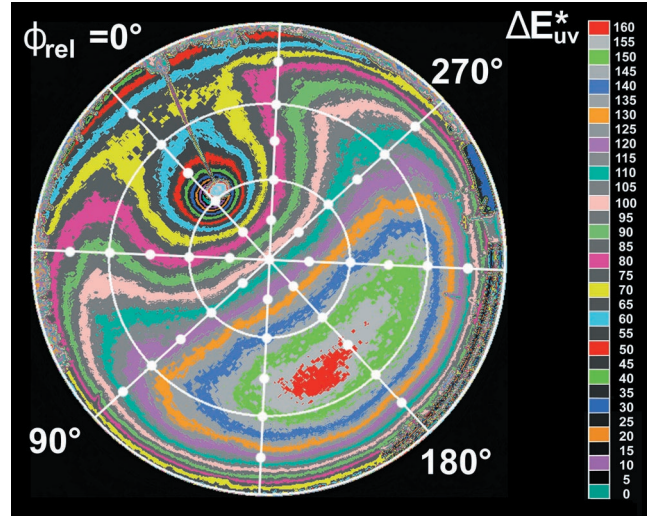

Fig. 2. Clear-sky color-difference map derived from Fig. 1. Overlaid on this map are the solar meridian (or clear-sky principal plane) with $\phi_{rel} = 0°$ and three meridians corresponding to $\phi_{rel} = 45°$, $90°$, and $315°$. Because we are looking up at the zenith rather than down at the nadir, ϕ_{rel} increases counterclockwise in this figure. Each map contour spans 5 units of the CIELUV color difference ΔE_{uv}^*. The most chromatic skylight colors are plotted in red ($\Delta E_{uv}^* = 160$) near $h = 45°$, $\phi_{rel} = 180°$; the least-chromatic skylight colors ($\Delta E_{uv}^* = 0$) are near the Sun.

L^*, u^*, v^* are the CIELUV space's orthogonal coordinates, and ΔL^*, Δu^*, Δv^* are the corresponding differences between coordinates of the two light sources being compared. Note that 3–5 CIELUV color-difference units are often taken to be 1 JND. Once again we use a 2% difference in luminance L_v as the luminance JND for photopic vision.

5. Asymmetry Results

Our first fish-eye photograph of a cloudless sky is Fig. 1, which was taken on 21 May 2000 when $h_0 = 60.0°$. The dark oval at h_0 is the sun shield described above. In Fig. 2 and subsequent figures, we indicate the Sun's position and selected h, ϕ_{rel} by overlaying a polar-coordinate system on the fish-eye views. This white overlay will be useful in visually identifying skylight color and luminance asymmetries, and it includes the horizon; the $h = 30°$ and $60°$ almucantars; the zenith; the solar meridian ($\phi_{rel} = 0°$); and $\phi_{rel} = 45°$, $90°$, and $315°$. Because the overlay's dots indicate the 44 h, ϕ_{rel} where we made our earlier spectroradiometer measurements,[13] the overlay also aids comparison with that study. Note that because we included the zenith in each of four meridional radiometer scans, only 41 separate dots appear in Fig. 2. Each of these four zenith spectra was acquired 6 min. apart,[13] which at small h_0 is long enough to produce perceptible changes in skylight color and luminance. Furthermore, ϕ_{rel} increases counterclockwise in Fig. 2, since we are looking up at the zenith, rather than down at the nadir.

In Fig. 2 we plot u^*, v^* calculated from our digital-image analysis of Fig. 1, but we do so in the form of a CIELUV color-difference map. Specifically, each gray band or color band in Fig. 2 corresponds to $\Delta E_{uv}^* = 5$ color-difference units; the most chromatic skylight colors are plotted in red near $h = 45°$, $\phi_{rel} = 180°$. So if a pair of GSV directions are plotted in different colors in Fig. 2, then their $\Delta E_{uv}^* > 5$, and their combined color and luminance differences exceed 1 JND. Because color changes smoothly as we look across the clear sky, this final statement does not imply that *adjoining* patches of sky in Fig. 2's different map bands differ perceptibly from one another. For an example of GSV differences in Fig. 2, compare the magenta band at $h = 30°$, $\phi_{rel} = 315°$ with the green band at $h = 30°$, $\phi_{rel} = 45°$. Because $\Delta E_{uv}^* \sim 10$ between these two GSV directions, the corresponding patches of clear sky in Fig. 1 would have different colors if compared side by side. Unlike the chameleon, sadly we cannot roll our eyes independent of each other in order to make simultaneous foveal comparisons of such disparate GSV directions. However, if we carefully aim a small mirror outdoors or juxtapose digital-image samples indoors, then we can see these differences in sky color.

What happens if we eliminate color from the clear sky and simply view it in shades of gray? In other words, if we ignore color can we still detect clear-sky asymmetries? Part of the answer comes from Fig. 3, which is a map of Fig. 1's luminances L_v. As with color differences, we find that this clear sky does indeed have perceptible luminance asymmetries. In Fig. 3, each gray band or color band spans a range of luminances $\Delta L_v = 2\%$; the darkest skylight colors are plotted in red near $h = 45°$, $\phi_{rel} = 180°$. For an example of suprathreshold luminance asymmetries in Fig. 3, compare the GSV directions $h = 30°$, $\phi_{rel} =$
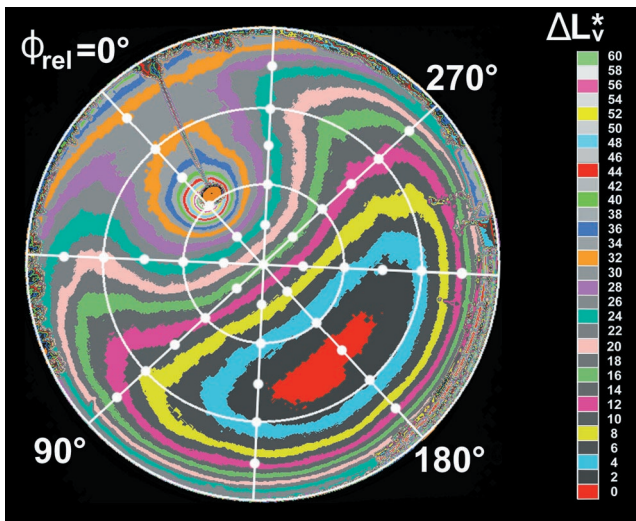
Fig. 3. Clear-sky luminance map derived from Fig. 1. Each map contour spans a range of luminances $\Delta L_v = 2\%$. The darkest skylight colors ($\Delta L_v = 0\%$) are plotted in red near $h = 45°$, $\phi_{rel} = 180°$; the brightest skylight colors ($\Delta L_v = 60\%$) are near the Sun.

Fig. 4. Fish-eye photograph of a clear sky in Granada, Spain, on 9 April 2001 at 18:50 UTC. Solar elevation $h_0 = -2.1°$ (i.e., during civil twilight), and the photograph is centered on the zenith.

315° (cyan band) and $h = 30°$, $\phi_{rel} = 45°$ (pink band). For this pair of directions $\Delta L_v \sim 3\%$, a small but clearly distinguishable difference. In fact, Table 1's ΔL_v statistics show that perceptible GSV luminance differences are the rule, rather than the exception, in Fig. 1: Its mean ΔL_v is nearly 4.3 times our nominal threshold value.

Direct visual comparisons suggest that luminance does not outweigh color in defining the clear sky's asymmetries. Using a colorimetrically calibrated color monitor and a digital image of Fig. 1, we juxtaposed pairs of color swatches corresponding to all its GSV directions. Of these thousands of GSV color pairs, we judged that 33% were visibly different and that most of these pairs appeared to differ in color rather than brightness. Although this judgment is necessarily subjective, visual interpretation is, after all, our ultimate benchmark here. Table 1 also shows that color differences matter in causing GSV asymmetries: the luminance-weighted chromaticity difference $\Delta u^*v^* \{= [(\Delta u^*)^2 + (\Delta v^*)^2]^{1/2}\}$ is a sig-
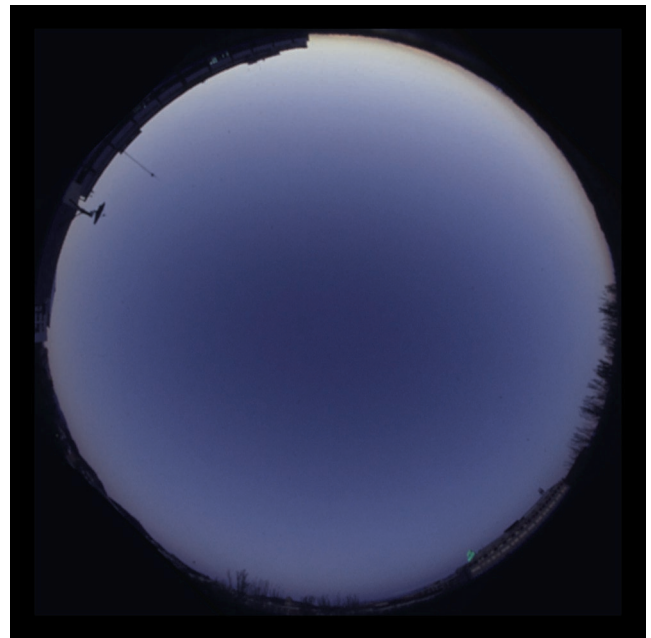
nificant fraction of the total stimulus difference ΔE_{uv}^* for Fig. 1.

Because surface reflectance spectra do not vary systematically within 40 km of Granada, our observed skylight asymmetries are unlikely to arise from variations in ground reflection. Furthermore, these asymmetries can largely disappear in <24 hr (see Section 6), something that cannot be explained by wholesale changes in surface reflectance. Instead, our clear-sky color and luminance asymmetries are likelier to be caused by local inhomogeneities in the kind and concentration of tropospheric aerosols. If surface sources of aerosols contribute to this variability across ϕ_{rel}, one plausible explanation for it would be that Granada has considerable arable land to its west, but much less in other directions. The city has no significant sources of industrial aerosols.

Our second clear-sky photograph is Fig. 4, which

Table 1. Summary Statistics for ΔL_v (%), Δu^*v^*, and ΔE_{uv}^* in Figs. 1, 4, and 7[a]

Figure No. and CIELUV Variable	n	$\bar{x}$	s	10th percentile	90th percentile
Fig. 1 ΔL_v (%)	139955	8.597	23.734	0.242	20.716
Fig. 4 ΔL_v (%)	136833	13.522	51.362	0.251	22.294
Fig. 7 ΔL_v (%)	146867	8.374	26.543	0.280	13.742
Fig. 1 Δu^*v^*	139955	3.584	7.454	0.274	10.080
Fig. 4 Δu^*v^*	136833	3.602	7.955	0.265	8.653
Fig. 7 Δu^*v^*	146867	3.146	5.734	0.258	7.456
Fig. 1 ΔE_{uv}^*	139955	5.039	9.946	0.356	16.412
Fig. 4 ΔE_{uv}^*	136833	5.375	12.250	0.398	13.221
Fig. 7 ΔE_{uv}^*	146867	4.381	8.668	0.356	10.271

[a]These statistics are calculated over n pairs of GSV clear-sky pixels, with each of the original L^*, u^*, and v^* values first being smoothed over its 8×8 pixel neighborhood. For all variables, $\bar{x}$ and s are the sample mean and standard deviation, respectively. Variable Δu^*v^* is a CIELUV luminance-weighted chromaticity difference and is given by $\Delta u^*v^* = [(\Delta u^*)^2 + (\Delta v^*)^2]^{1/2}$.

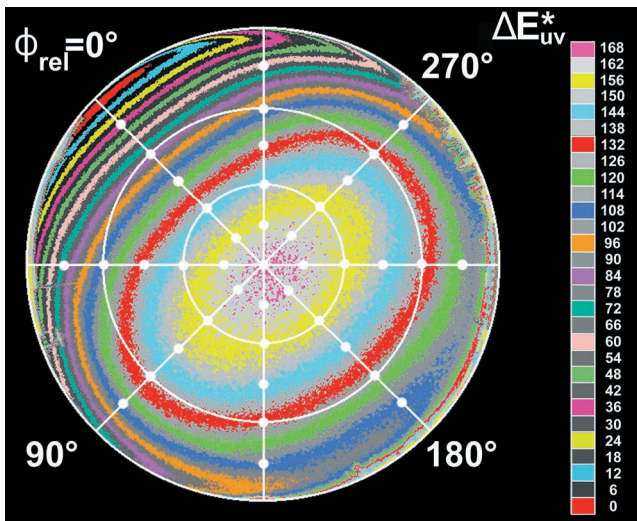Fig. 5. Clear-sky color-difference map derived from Fig. 4, with each map contour spanning $\Delta E_{uv}^* = 6$.

Fig. 7. Fish-eye photograph of a clear sky in Granada, Spain, on 10 April 2001 at 15:36 UTC. Solar elevation $h_0 = 36.1°$, and the photograph is centered on the zenith.

was taken during civil twilight ($h_0 = -2.1°$) on 9 April 2001. This sky, along with its corresponding color and luminance maps (Figs. 5 and 6, respectively), shows just how distinct skylight asymmetries can be. In these figures we do not use the below-horizon Sun to identify the principal plane, but instead we locate it by combining solar ephemeris calculations with the known azimuths of topographic features. In fact, even a cursory examination of Figs. 5 and 6 reveals substantially greater color and luminance asymmetries than in Figs. 2 and 3. Table 1 shows that the mean ΔL_v for Fig. 4's GSV directions is ~1.5 times that for Fig. 1, and the means of both Δu^*v^* and ΔE_{uv}^* have increased in Fig. 4 (the ΔE_{uv}^* increase is statistically significant at the 0.1% level). The physical reason for these increases is that direct sunlight's long optical paths during twilight amplify any 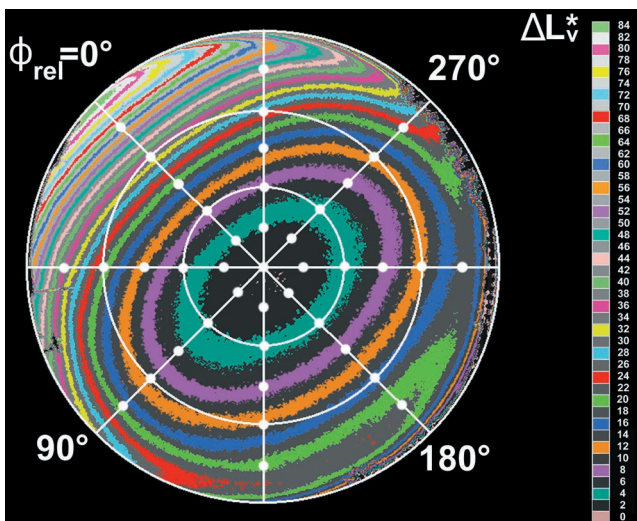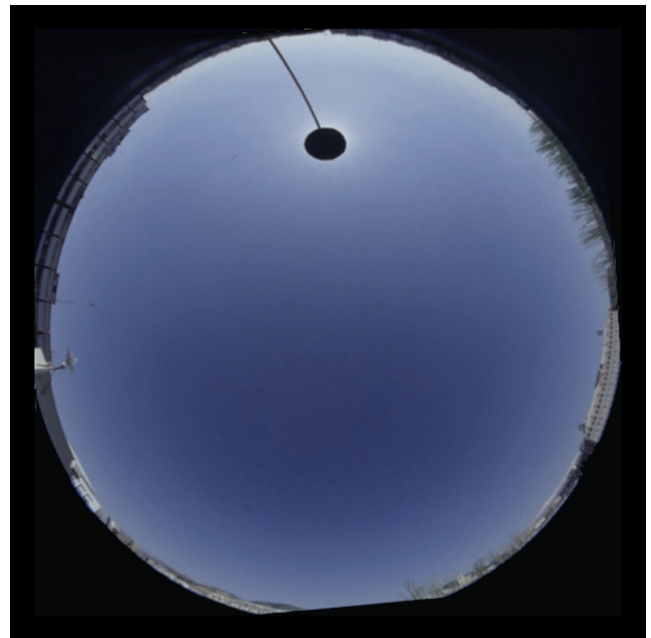differences in spectral scattering and absorption that are caused by horizontal inhomogeneities in the atmosphere.[11] This in turn increases skylight color and luminance asymmetries compared with the same atmosphere at higher h_0.

6. The Polarization Bugbear

The question of polarization-induced asymmetries quite rightly haunts any analysis of skylight color and luminance data. Here this question is, does the clear sky's high degree of linear polarization P cause spurious color and luminance differences in either our camera or spectroradiometers as they sample light from two GSV directions? For example, might instrument self-polarization or a polarization-dependent change in spectral sensitivity make a spectroradiometer produce nonexistent differences in chromaticity and luminance? In fact, there are both theoretical and observational reasons to think that any such spurious differences are negligible.

First, light transmitted through our PR-650 spectroradiometer's input optics is depolarized just before reaching the instrument's diffraction grating, thus avoiding measurement problems associated with both self-polarization and intrinsic polarization.[20,21] Similar precautions are taken within the LI-1800 spectroradiometer's optical chain. The fact that both instruments measured comparable skylight asymmetries in similar GSV directions strongly suggests that these differences are real. Second, since in principle P is the same for any given pair of GSV directions, polarization's effects on color and luminance should also be the same. Yet in practice, our earlier research shows that P itself is asymmetric about the solar meridian.[22] The least-complicated explanation for these observations is that *all three*

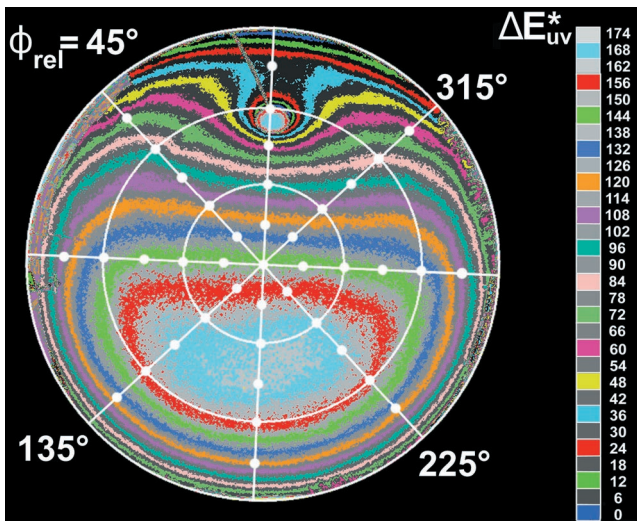Fig. 6. Clear-sky luminance map derived from Fig. 4, with each map contour spanning $\Delta L_v = 2\%$.

Fig. 8. Clear-sky color-difference map derived from Fig. 7, with each map contour spanning $\Delta E_{uv}^* = 6$.

skylight properties are distributed unevenly in the horizontally inhomogeneous volume of air above us.

But might not angular and spatial asymmetries in camera optics or film response explain what we see in Figs. 1–6? Although we cannot exclude such problems as confidently as we did for our spectroradiometers, Figs. 7–9 suggest that any photographic polarization artifacts are small at best. Figure 7 was taken just one day after the highly asymmetric Fig. 4, and our camera's and film's polarization responses were unchanged from Fig. 4. Yet Fig. 7's color and luminance maps (Figs. 8 and 9) indicate that its clear sky is much more symmetric than that in Fig. 4. This strong visual impression is confirmed by Table 1's data: Mean ΔE_{uv}^*, ΔL_v, and Δu^*v^* all decrease in Fig. 7 (at the 0.1% significance level), and the decrease in mean ΔE_{uv}^* is likely to be perceptible.
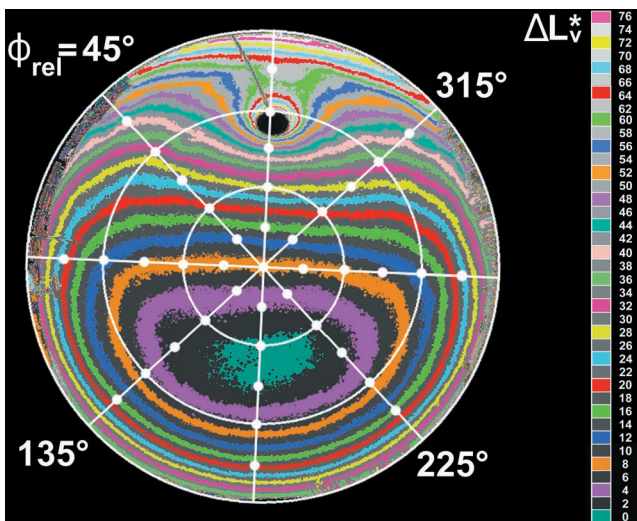

Fig. 9. Clear-sky luminance map derived from Fig. 7, with each map contour spanning $\Delta L_v = 2\%$.

In addition, all three means are smaller for Fig. 7 than for our other daytime image, Fig. 1.

These results make good physical sense. Compared with Fig. 1, the slightly bluer sky in Fig. 7 implies lower turbidity, thus moving its sky closer to the symmetric Rayleigh atmosphere and farther from one with asymmetries caused by, say, spatial variations in aerosol concentration. Thus we conclude that our measured color and luminance asymmetries are real, rather than artifacts. In fact, the simplest, most reasonable optical explanation for what we observe is that clear-sky color, luminance, and polarization asymmetries are natural corollaries of one other. In other words, when one kind of asymmetry is present, so are the other two.

7. Conclusions

Our purpose in this paper is to demonstrate the reality of clear-sky color and luminance asymmetries. Their persistence across a variety of measuring instruments and techniques strongly suggests that they are real, rather than instrument artifacts. Although space limitations here mean that we cannot be encyclopedic in offering examples, we do note that our analysis of two years of Granada clear-sky photographs firmly supports our earlier conclusion[13]: Perceptible skylight luminance and color asymmetries are the rule, rather than the exception, in real atmospheres.

Although the apparent dome of the clear sky may summon thoughts of celestial perfection and symmetry, our research shows something quite different. No matter how clear the sky may appear to us, on many days its color and luminance are asymmetric about the solar meridian. We are not claiming that every clear day is asymmetric, nor has our research progressed far enough to let us offer a thorough statistical analysis of the frequency of skylight asymmetries. Another logical next step in our ongoing research into the clear sky's visible structure[11,13,22–27] is to model these common asymmetries in ways that offer some basic physical insights into their causes.

References and Note

1. F. C. Hooper, A. P. Brunger, and C. S. Chan, "A clear sky model of diffuse sky radiance," J. Sol. Energy Eng. **109,** 9–14 (1987).
2. R. Perez, J. Michalsky, and R. Seals, "Modelling sky luminance angular distribution for real sky conditions: experimental evaluation of existing algorithms," J. Illum. Eng. Soc. **21,** 84–92 (1992).
3. F. M. F. Siala, M. A. Rosen, and F. C. Hooper, "Models for the directional distribution of the diffuse sky radiance," J. Sol. Energy Eng. **112,** 102–109 (1990).
4. C. R. Prasad, A. K. Inamdar, and H. P. Venkatesh, "Computation of diffuse radiation," Sol. Energy **39,** 521–532 (1987).
5. R. Perez, R. Seals, and J. Michalsky, "All-weather model for

sky luminance distribution—preliminary configuration and validation," Sol. Energy **50,** 235–245 (1993).

6. A. W. Harrison and C. A. Coombes, "Angular distribution of clear sky short wavelength radiance," Sol. Energy **40,** 57–63 (1988).

7. E. M. Winter, T. W. Metcalf, and L. B. Stotts, "Sky-radiance gradient measurements at narrow bands in the visible," Appl. Opt. **34,** 3681–3685 (1995).

8. G. Zibordi and K. J. Voss, "Geometrical and spectral distribution of sky radiance: comparison between simulations and field measurements," Remote Sens. Environ. **27,** 343–358 (1989).

9. C. Chain, D. Dumortier, and M. Fontoynont, "A comprehensive model of luminance, correlated colour temperature and spectral distribution of skylight: comparison with experimental data," Sol. Energy **65,** 285–295 (1999).

10. S. Sekine, "Spectral distributions of clear sky light and their chromaticities," J. Light Visual Environ. **15,** 23–32 (1991).

11. R. L. Lee, Jr., "Twilight and daytime colors of the clear sky," Appl. Opt. **33,** 4629–4638, 4959 (1994).

12. R. L. Lee, Jr., "Colorimetric calibration of a video digitizing system: algorithm and applications," Color Res. Appl. **13,** 180–186 (1988).

13. J. Hernández-Andrés, J. Romero, and R. L. Lee, Jr., "Colorimetric and spectroradiometric characteristics of narrow-field-of-view clear skylight in Granada, Spain," J. Opt. Soc. Am. A **18,** 412–420 (2001).

14. G. Wyszecki and W. S. Stiles, *Color Science: Concepts and Methods, Quantitative Data and Formulae* (Wiley, New York, 1982), pp. 306–310, 828–829.

15. LI-1800 spectroradiometer from LI-COR. Incorporated, 4421 Superior Street, Lincoln, Neb. 68504-1327.

16. PR-650 spectroradiometer from Photo Research, Incorporated, 9731 Topanga Canyon Place, Chatsworth, Calif. 91311.

17. Nikkor fish-eye lens from Nikon USA, 1300 Walt Whitman Road, Melville, New York 11747.

18. This particular lens is described in R. Kingslake, *A History of the Photographic Lens* (Academic, Boston, 1989), pp. 146–147. Although near-horizon skylight passes through a much greater thickness of its optical glass than does zenith skylight entering along its optical axis, this difference likely has negligible effects on our asymmetry results because spectral transmissivity in this lens is independent of rotation angle about its optical axis.

19. ASTM Committee E-12, "Standard practice for computing the colors of objects by using the CIE system (E 308-95), in ASTM standards on color and appearance measurements" (American Society for Testing and Materials, Philadelphia, Pa., 1996), pp. 262–263.

20. Photo Research, Incorporated, *PR-650 SpectraScan Spectra-Colorimeter Operating Manual, Software Version 1.10* (Photo Research, Incorporated, Chatsworth, Calif., 1996), Sec. 3, p. 4.

21. R. Gerharz, "Self polarization in refractive systems," Optik **43,** 471–485 (1975).

22. R. L. Lee, Jr., "Digital imaging of clear-sky polarization," Appl. Opt. **37,** 1465–1476 (1998).

23. R. L. Lee, Jr., "Horizon brightness revisited: measurements and a model of clear-sky radiances," Appl. Opt. **33,** 4620–4628, 4959 (1994).

24. J. Romero, A. García-Beltrán, and J. Hernández-Andrés, "Linear bases for representation of natural and artificial illuminants," J. Opt. Soc. Am. A **14,** 1007–1014 (1997).

25. J. Hernández-Andrés, J. Romero, A. García-Beltrán, and J. L. Nieves, "Testing linear models on spectral daylight measurements," Appl. Opt. **37,** 971–977 (1998).

26. J. Hernández-Andrés, R. L. Lee, Jr., and J. Romero, "Calculating correlated color temperatures across the entire gamut of daylight and skylight chromaticities," Appl. Opt. **38,** 5703–5709 (1999).

27. J. Hernández-Andrés, J. Romero, J. L. Nieves, and R. L. Lee, Jr., "Color and spectral analysis of daylight in southern Europe," J. Opt. Soc. Am. A **18,** 1325–1335 (2001).